Acta Physiologiae Plantarum (2017) 39:274
https://doi.org/10.1007/s11738-017-2571-x

ORIGINAL ARTICLE

Transcriptome analysis of pale-green leaf rice reveals photosynthetic regulatory pathways

Xia Zhao[1,2] · Baohua Feng[1] · Tingting Chen[1] · Caixia Zhang[1] · Longxing Tao[1] · Guanfu Fu[1]

Received: 16 December 2016 / Revised: 5 November 2017 / Accepted: 7 November 2017

Abstract

Chlorophyll metabolic pathways and chloroplast development have been studied systematically by both biochemical and genetic approaches. However, the effect of them on photosynthesis has not been thoroughly elucidated to date. To gain expression profiles of genes involved in crucial pathways and regulators of photosynthetic metabolism in rice seedling, biochemical characteristics and transcriptome of two rice genotypes were compared. Zhefu802 and Chl-8 are the recurrent parent (dark-green leaf) and its near-isogenic lines (pale-green leaf), respectively. The net photosynthetic rate, F_v/F_m and Φ_{PSII} of Chl-8 were markedly higher than those of Zhefu802, although the chlorophyll content of Chl-8 was approximately one-third of Zhefu802. In this research, photosynthesis is controlled by delicate but complex genetic networks. In addition to DEGs directly involved in photosynthesis, DEGs involved in response to oxidative stress, energy metabolism and nitrate metabolism co-regulated photosynthetic efficiency in rice. DEGs categorized to signal transduction supported the regulation. Chloroplasts possessing an abundant thylakoid membrane system were not favored to photosynthesis. Five DEGs assigned to chloroplast category (GO:0009507) was genetic basis of difference on thylakoid membrane. Meanwhile, suitable chlorophyll content, chlorophyll *a*:*b* and ratio of chlorophyll to carotenoid, which caused by leaf and chloroplast structure, also promoted high photosynthesis. In summary, high photosynthetic efficiency involves coordinated regulation of the synthesis of multiple pigments, chloroplast development, response to oxidative stress, energy metabolism and nitrate metabolism.

Keywords Transcriptome analysis · Chlorophyll · Chloroplast development · Photosynthesis · Rice (*Oryza sativa* L.) · Oxidative stress

Introduction

Rice is a most important staple food crop, supplying a fifth of the world's dietary energy. Yield of rice is determined by the accumulated photosynthetic assimilates over the entire growing season that are distributed into the caryopses. It has been thought that cereal yield is currently approaching a plateau and further increases in yield necessitate improvement in photosynthesis (Gu et al. 2014; Long et al. 2015). There is compelling interest in improving photosynthetic efficiency through change of several morphological, physiological and biochemical traits in leaves. Photosynthesis is complex and involves an interplay of a vast array of genes. Although many researches on the mechanism of photosynthesis have been conducted, there are still large gaps in our knowledge of synthetic improvement of photosynthetic efficiency in crops (Sage and Sage 2009; Gu et al. 2014; Long et al. 2015). Photosynthesis is divided into two phases, defined as the light and dark reactions. The light reaction includes the harvest of light energy by chlorophyll and associated pigments, water splitting, and electron transport to reduce NADP and provide the proton gradient across thylakoid membrane

Communicated by Y. Wang.

Xia Zhao and Baohua Feng contributed equally to this paper.

Electronic supplementary material The online version of this article (https://doi.org/10.1007/s11738-017-2571-x) contains supplementary material, which is available to authorized users.

✉ Longxing Tao
lxtao@fy.hz.zj.cn

✉ Guanfu Fu
fugf1981@sina.com

[1] State Key Laboratory of Rice Biology, China National Rice Research Institute, Hangzhou 310006, Zhejiang, China

[2] Yibin University, Yibin 644000, Sichuan, China

Published online: 14 November 2017

that powers phosphorylation of ADP. In the dark reaction, the resulting NADPH and ATP power the assimilation of carbon dioxide into carbohydrate products (Long et al. 2015).

As previously mentioned, chlorophyll and associated pigments capture light energy and transfer the excitation energy to reaction center in photosynthetic organisms. By 2015, more than 182 leaf color genes had been identified, and about 30 genes of these genes were derived from rice (Liu et al. 2015). It was demonstrated that these genes were involved in the chlorophyll metabolism and chloroplast development (Kong et al. 2016). Sakuraba et al. (2013) identified *OsPORB*, which encodes protochlorophyllide oxidoreductase B, as an essential for maintaining light-dependent chlorophyll synthesis throughout leaf development. Wu et al. (2007) isolated yellow-green leaf 1 (*ygl1*), a rice chlorophyll-deficient mutant, which displayed yellow-green leaves in young seedling with decreased chlorophyll content, increased level of tetrapyrrole intermediates, and delayed chloroplast development. Wang et al. (2013) isolated a rice mutant named yellow-green leaf 2 (*ygl2*) which showed heme oxygenase 1 deficiency, Heme oxygenase 1 converts heme to BV-IXα with the release of iron (Fe^{2+}) and carbon monoxide. In contrast to its essential energy-harvesting role, chlorophyll and its intermediate derivatives can also interact with oxygen molecules to give rise to toxic singlet oxygen radicals. Therefore, chloroplast development and maintenance require exact control of chlorophyll synthesis (Sakuraba et al. 2013). Greater content of chlorophyll does not necessarily mean higher rates of photosynthesis, and specifically, low chlorophyll rice plants with high photosynthesis were found (Wang et al. 2012). An identical trend was also found in these experiments, even though the chlorophyll content of Chl-8 was significantly less than that of Zhefu802. The net photosynthetic rate (Pn) of Chl-8 was markedly higher than that of Zhefu802. The chlorophyll metabolism and chloroplast development mechanism have been studied systematically by both biochemical and genetic approaches. However, the effect of chlorophyll metabolism on photosynthesis is still vague.

RNA-Seq analysis based on next generation sequencing was applied extensively for transcriptome analysis. RNA-Seq analysis can cover the complete transcriptome of a sample (Wakasa et al. 2014; Cao et al. 2016). Thus, comparison of comprehensive expression profiles based on RNA-Seq analysis can reveal general genetic regulatory mechanisms involved in pigment metabolism and photosynthesis. Wu et al. (2016) reported that *Baijiguan*, a tea cultivar, shows a yellow leaf phenotype, decreased chlorophyll content, and aberrant chloroplast structures under high light intensity, and differentially expressed genes were predominantly involved in the active oxygen species scavenging system, chloroplast development, photosynthetic pigment synthesis, secondary metabolism and circadian systems. RNA-Seq analysis also revealed that, in mutants of *Anthurium andraeanum* 'Sonate', chloroplast ultrastructure and multiple pigments biosynthesis together impacted the leaf color formation (Yang et al. 2015). However, little is known regarding general genetic regulatory mechanisms involved in photosynthesis in rice.

In our research, we compared the biochemical characteristics of two rice genotypes, Zhefu802, the recurrent parent (dark-green leaf cultivar), and its near-isogenic lines, Chl-8 (a pale-green leaf cultivar). The gas change, chlorophyll fluorescence analysis, generation of reactive oxygen species and ultrastructure of the chloroplasts of the two cultivars were studied. Furthermore, to gain expression profiles of genes involved in crucial pathways and regulators of photosynthetic metabolism in rice seedling, we used RNA-Seq analysis to investigate gene expression in the two cultivars. The use of the pale-green leaf variety with high photosynthesis activity for study is complementary to previous work conducted on typical green leaf and provides novel information regarding the molecular mechanism for high photosynthetic efficiency in rice.

Materials and methods

Plant materials

Two rice near-isogenic lines, Zhefu802 (recurrent parent) and Chl-8, were selected for this research. Zhefu802 possesses dark-green leaf, and Chl-8 possesses pale-green leaf. Pre-germinated seeds of each genotype were sown in 5-l black buckets filled with 3 kg soil. A series of experiments were conducted in a growth chamber with 12 h day/night (d/n) at 75%/80% (d/n) relative humidity and 30 °C/23 °C (d/n) temperatures. The seventh leaves (youngest fully expanded leaves) of seedlings were selected to perform RNA-Seq analysis and to measure gas exchange and subsequent measurements.

Chlorophyll content analysis

According to the method described by Sartory and Grobbelaar (1984), Chlorophyll *a* and *b* was extracted, and then their contents were quantified. 0.1 g leaf fragments were immersed in 20 ml 95% (v/v) ethanol for 48 h. Absorbance of 665, 649 and 470 nm were measured by spectrophotometer. Chlorophyll *a* and *b* concentrations were calculated according to these formulas: chlorophyll *a* (C_a μg ml^{-1}) = 13.95 (A_{665}) − 6.88 (A_{649}); chlorophyll *b* (C_b μg ml^{-1}) = 24.96 (A_{649}) − 7.32 (A_{665}); carotenoid (μg ml^{-1}) = (1000 (A_{470}) − 2.05C_a − 114.8C_b)/245.

Gas exchange measurement

The Pn was determined by an infrared gas analyzer-based portable photosynthesis system (LI-6400; Li-Cor, Lincoln, NE, USA) mounted with a red/blue LED light source (6400-02B; Li-Cor) on the seventh leaves. During the measurement, the CO_2 concentration was 400 µl l^{-1}, the light intensity was 1000 µmol m^{-2} s^{-1} and leaf temperature was 30 °C.

Transverse sections of leaves

Leaves were sampled after illumination for 1 h. The segments of leaf samples were fixed in 2.5% (v/v) glutaraldehyde and conserved at 4 °C to make the paraffin section. Leaf cross-sections were stained with safranin and fast green, and observed at 400× magnification with Leica DM1000 (Leica Microsystems, Ltd, Germany). The structure and arrangement of multiple cells on the transverse sections of leaves were observed in light micrographs mounted with a digital camera (Ruzin 1999).

Ultrastructure of chloroplast

Leaves were sampled after illumination for 1 h. The segments of leaf samples were fixed in 2.5% (v/v) glutaraldehyde and conserved at 4 °C. The segments of leaf samples were immersed in 1% (w/v) osmium tetroxide at 4 °C for at least 10 h. The treated samples were dehydrated in a graded acetone series and embedded in Spurr's resin (Ladd). 40-nm ultrathin sections cut with a diamond knife on the ultramicrotome were prepared for the observation of transmission electron microscopy of chloroplast ultrastructure (Leica Ultracut R) and ultrathin sections stained using uranyl acetate and lead citrate double staining. Chloroplast ultrastructure was observed and electron micrographs were taken under an electron microscope mounted with a digital camera (Bozzola and Russell 1999).

Induction of chlorophyll fluorescence

Induction of chlorophyll fluorescence was measured by PAM-2500,a portable Chlorophyll fluorometer (Walz Heinz GmbH, Effeltrich, Germany). The leaves were adapted in the dark for 30 min before measurement. The minimum fluorescence (F_o) was examined using measuring light. To obtain the maximum fluorescence (F_m), a 0.8-s pulse of saturating light (8000 mol m^{-2} s^{-1} red light) was applied after 30 min in darkness. Maximum quantum efficiency of PSII (F_v/F_m) was defined as $(F_m - F_o)/F_m$. The steady-state chlorophyll fluorescence (F_s) was measured after 5 min actinic light application. In the light-adapted state, a saturating pulse was applied to measure F'_m. Switching off the actinic light for 2 s after the saturating pulse and applying far-red (FR) light were to measure F'_o. Photochemistry quench (qP) was calculated by $1 - (F_s - F'_o)/(F'_m - F'_o)$. Actual quantum efficiency of PSII (Φ_{PSII}) was calculated by $(F'_m - F_s)/F'_m$. Non-photochemical quenching (NPQ) was calculated by $F_m/F'_m - 1$ (Maxwell and Johnson 2000).

Determination of malondialdehyde (MDA) content

According to the method of Dionisio-Sese and Tobita (1998), the concentration of MDA was measured. Leaf samples (0.3 g) were soaked in liquid nitrogen and ground with a mortar and pestle. 5 ml ice-cold 10% (w/v) trichloroacetic acid was added to mortar and leaf powder was ground to homogenate. The homogenate was centrifuged for 15 min at 10,000×*g*, and 2 ml supernatant was mixed with 2 ml 0.67% (w/v) thiobarbituric acid solution containing 10% (w/v) trichloroacetic acid. The mixture was heated in the thermostatic water bath at 100 °C for 30 min, and the reaction was stopped via ice bath. Absorbance of 450, 532, and 600 nm was measured by spectrophotometer, and then the MDA concentration was calculated as $6.45 \times (A_{532} - A_{600} - 0.56 \times A_{450}$.

Hydrogen peroxide determination

The youngest fully expanded leaves were cut, placed in 1 mg ml^{-1} 3,3′-diaminobenzidine-HCl (pH 3.8), incubated in the growth chamber for 1 h in dark at 25 °C, and incubated for 12 h in light. The leaves were cleared with distilled water and immersed in boiling ethanol for 10 min to dissolve pigments. H_2O_2 was visualized as a reddish-brown coloration and the picture was taken with a digital camera (Thordal-Christensen et al. 1997).

Superoxide anion (O_2^-) measurement

The rate of O_2^- production was examined by the method of Chaitanya and Naithani (1994). 0.3 g frozen leaf samples were ground with a mortar and pestle in liquid nitrogen. 100 mM sodium–phosphate buffer (pH 7.2) containing 1 mM diethyl dithiocarbamate was added to mortar to obtain homogenate. Diethyl dithiocarbamate can make superoxide dismutase (SOD) inactivation. The homogenate was centrifuged for 20 min at 13,000×*g*, the supernatant was conducted to determine the productive rate of O_2^- via its capacity to reduce nitroblue tetrazolium. The reaction mixture (3 ml) contained the supernatant of a leaf sample, 1 mM diethyl thiocarbamate, 100 mM sodium phosphate buffer (pH 7.2) and 0.25 mM nitroblue tetrazolium. Absorbance of 540 nm was measured by spectrophotometer (Lambda 25, Perkin Elamer, USA) (Boveris 1984).

RNA extraction and sequencing

RNA was extracted from the youngest fully developed leaves after 2 h illumination using TriZol (Invitrogen), cleaned and DNAse1-treated using the Sigma Plant Total RNA kit (Sigma Aldrich). The quality of the resulting RNA was evaluated via the Agilent 2100 Bioanalyzer. To construct cDNA library, a TruSeq™ RNA Sample Preparation Kit was used to treat total resulting RNA from samples. To product 125 bp PE reads for transcriptome sequencing on an Illumina High-Seq 2500 platform, sequencing was conducted on each library via a commercial service provider (biomarker, Beijing, China). The analysis was performed with three biological replicates.

Transcript quantification and differential gene expression analysis

Publicly available tools were used to analyze raw sequences in FASTQ format gained from the Illumina platform. Low-quality bases ($Q < 15$) were trimmed from both ends of the sequences via a customized program, and Cutadapt was used to trim the adapters. The sequences were mapped to the complete set of CDS from Rice_9311 (http://rice.genomics.org.cn/rice2/link/download.jsp) using TopHat2 (Kim et al. 2013). Reference-based assembly of the reads was performed using Cufflinks and Cuffmerge (http://cufflinks.cbcb.umd.edu/). Single Nucleotide Polymorphism (SNP) detection via SAMtools was performed using the following quality and significance filters: the score from TopHat2 alignment ≥ 50, interval between single-base mismatch ≥ 5 bases, variant calling quality value ≥ 20, sequencing depth ≥ 5× and ≤ 100× (Li et al. 2009). The expression level of each gene was defined as the fragments per transcript kilobase per million fragments mapped (FPKM) value; FPKM = cDNA fragments/(mapped fragments × transcript length). All pairwise comparisons between Zhefu802 and Chl-8 were conducted using DESeq (Anders and Huber 2010), using the default normalization method and differentially expressed genes (DEGs) were identified according to Benjamini–Hochberg corrected P value ≤ 0.01 and fold change ≥ 2 (Benjamini and Hochberg 1995). A GO term was distributed to each gene according to the GO annotations for biological process in RAP-DB. (The Rice Annotation Project Database, http://rapdb.dna.affrc.go.jp).

Validation of RNA-Seq data by quantitative RT-PCR

To validate the results from the RNA-Seq experiment, ten of the key DEGs involved in photosynthesis-related processes were selected for qRT-PCR analysis. Total RNA was extracted from 0.1 g leaf samples via TRIpure reagent (Aidlab Biotechnologies, Beijing, China). Total RNA was converted into the first-strand cDNA using ReverTra Ace qPCR RT Master Mix (TOYOBO, Shanghai, China) with oligo (dT) as a primer. The resulting cDNA was used as a template for quantitative PCR amplification in a Thermal Cycler Dice Real Time System II (TaKaRa Biotechnology, Dalian, China) with the SYBR Green I (TOYOBO) as a fluorescent reporter. All primers are listed in table S1 (Feng et al. 2013). Rice *ubiquitin1* was used to normalize the detection threshold cycle for each reaction. Relative expression levels were calculated with ΔΔCT method.

Statistical analysis

All data were processed with SAS 9.0. Tukey's least significant difference (LSD) at a probability level of 5% was used to compare the differences within treatments and genotypes.

Results

Chlorophyll content, carotenoid content and structural basis of leaves

Zhefu802 plants displayed the dark-green leaf phenotype, whereas Chl-8 plants showed the faded green leaf phenotype shown in Fig. 1. To characterize the leaf color phenotypes of the two cultivars, their respective chlorophyll and carotenoid contents were determined (Table 1). The Chlorophyll *a*, Chlorophyll *b*, and carotenoid contents of Chl-8 were significantly lower than those of Zhefu802; however, the values of chlorophyll *a*:*b* and carotenoid:chlorophyll in Chl-8 were significantly higher than those in Zhefu802.

To characterize the structural basis of the leaf color phenotype, cross-sections of rice leaf and ultrastructures of chloroplast were compared (Figs. 2, 3). There was a decrease in leaf thickness of Chl-8 compared to Zhefu802. No significant differences in mesophyll tissue thickness and size of mesophyll cells between the two cultivars were observed (Fig. 2). Chloroplasts in Zhefu802 developed an abundant membrane system with grana connected by stroma lamellae (Fig. 3b). However, the appressed and non-appressed thylakoid membrane was less dense in Chl-8 (Fig. 3d).

Gas change and generation of toxic oxides

The Pn of Chl-8 was higher than Zhefu802 by approximately 25.57%, and Chl-8 also had significantly higher dry weight of shoot (Fig. 4a, b). The concentrations of MDA and the productive rate of superoxide (O^{2-}) in Chl-8 were significantly lower than that in Zhefu802. Figure 4d provides an overview of H_2O_2 concentration in the leaves of the two varieties. Deeper color, representing high H_2O_2 concentration in leaves, was observed in Zhefu802 compared to Chl-8.

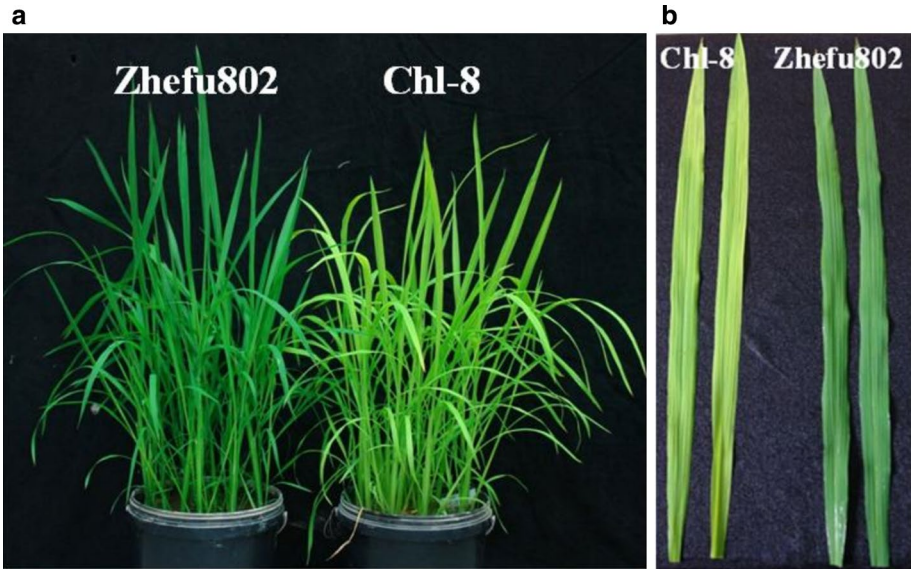

Fig. 1 Growth performance (**a**) and leaf color (**b**) of Zhefu702 and Chl-8 in the seven leaf stage

Table 1 Chlorophyll and carotenoid content in Zhefu802 and Chl-8

Material	Chl *a* (mg g^{-1})	Chl *b* (mg g^{-1})	Carotenoid (mg g^{-1})	Chl *a*:*b*	Carotenoid:Chl
Zhefu802	3.10a	1.33a	0.51a	2.34b	0.12b
Chl-8	0.85b	0.09b	0.26b	9.70a	0.28a

Different lower-case letters indicate statistically significant differences ($P < 0.05$) between Zhefu802 and Chl-8

Chlorophyll fluorescence analysis

To investigate the ability to generate electron flow via the absorption of light energy in photosynthetic system II, chlorophyll fluorescence analysis was conducted via PAM-2500. Table 2 shows the values of F_v/F_m, Φ_{PSII}, 1-qP and NPQ of the two varieties. There were significantly higher levels of F_v/F_m, Φ_{PSII} and NPQ and a lower level of 1-qP in the leaves of Chl-8, indicating a much more robust ability to generate the electron transport and dissipated excessive excited energy via heat.

Transcriptome analysis

In total, we obtained 37.96 Gb of clean data from paired-end reads, with a *Q*30 percentage of over 86.65% (Table 3). We determined that 84.37–85.55% of clean data aligned to the complete set of CDS from Rice_9311 (http://rice.genomics.org.cn/rice2/link/download.jsp). Approximately 400 million quality evaluated reads per cDNA library were aligned to the rice genome and used for further analysis (Table 4). Low level of abundance of SNP in 12 chromosomes indicated the presence of a high degree of genetic similarity and less potential DEGs between Zhefu802 and Chl-8 (Table 5). The expressions of 17,903 genes were investigated in this RNA sequencing analysis and 1094 novel transcripts were detected.

The comparison of Zhefu802 with Chl-8 was obtained from three biological replications of RNA sequencing analysis (Fig. 5). Pearson's correlation coefficients between biological replications were over 95.28%. A total of 140 DEGs were detected (fold change ≥ 2; $P \leq 0.05$), including 76 up-regulated genes and 64 down-regulated genes (Fig. 5a). To gain insight into the differentiation of transcript expression profiles between Zhefu802 and Chl-8, we illustrated expression patterns with a heat map obtained via hierarchical cluster analysis (Fig. 5b). This clustering revealed the relatedness of the various transcripts.

Gene ontology (GO) classification was used to distribute the functional categories of RAP-annotated. GO terms with more than five DEGs are listed in Table 6. Within the biological process category, oxidation–reduction process (GO:0055114), regulation of transcription (GO:0006355), and transport (GO:0006810) were the top three GO terms. The top three GO terms in the cellular component category included the cytoplasmic membrane-bounded vesicle (GO:0016023), nucleus (GO:0005634), integral to membrane (GO:0016021). The most highly represented molecular function terms were ATP binding (GO:0005524), protein serine/threonine kinase activity (GO:0004674),

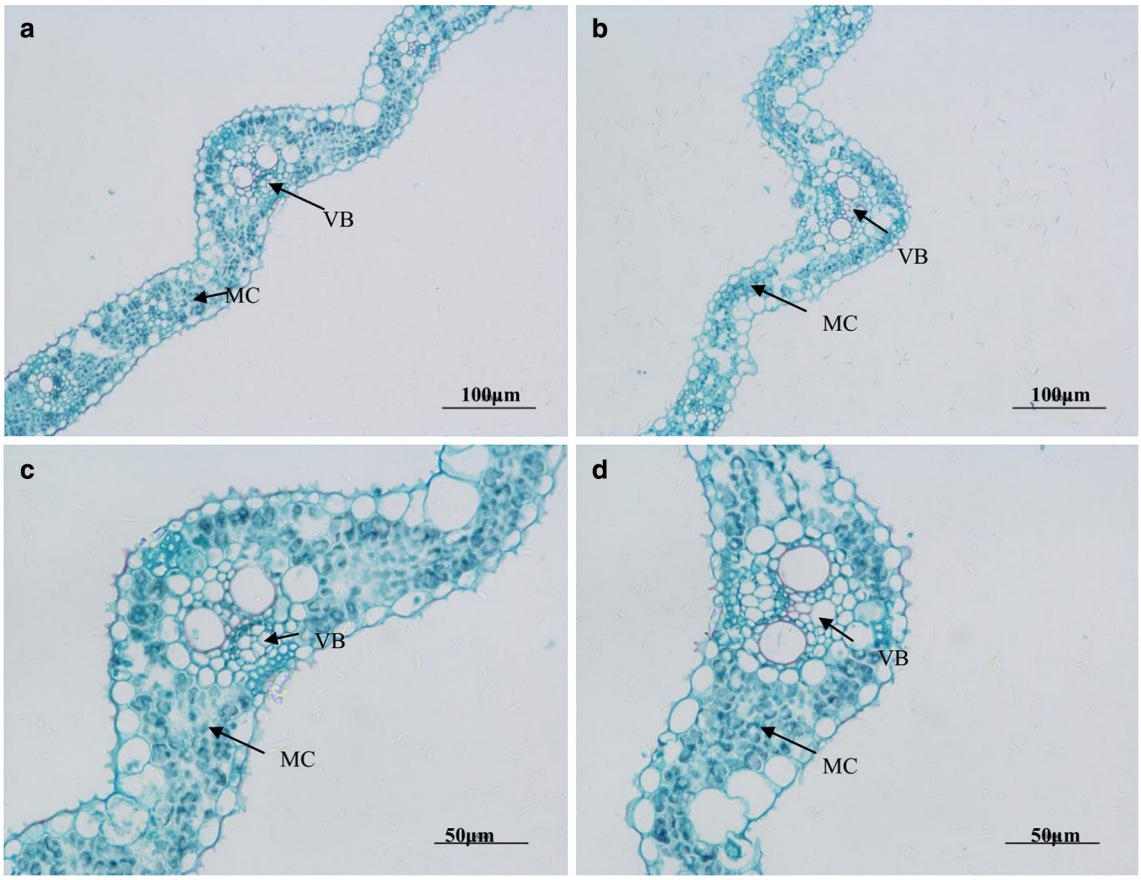

Fig. 2 Cross-sections of the youngest fully expanded leaves of Zhefu802 and Chl-8. **a**, **c** Cross-sections of Zhefu802 leaf. **b**, **d** Cross-sections of Chl-8 leaf. MC: mesophyll cell, VB: vascular bundle

protein binding (GO:0005515) and oxidoreductase activity (GO:0016705). Kolmogorov–Smirnov test showed oxidation–reduction process (GO:0055114) was most significant. Five DEGs were assigned to chloroplast category (GO:0009507), which is in line with the significant differences regarding the structures of leaf and ultrastructures of chloroplast between Zhefu802 and Chl-8. These results suggest that the development of the leaf and thylakoid membrane plays a key role in the regulation of photosynthetic efficiency.

All DEGs were matched to the sense sequences in the Rice Annotation Project Database (RAP-DB, http://rapdb.dna.affrc.go.jp). Following the functional categories given by GO and Annotation in RAP-DB, we manually classified these genes into 14 major categories, including response to oxidative stress, carbohydrate metabolism, cytochrome p450, photosynthesis, ATP metabolism, phytohormone, response to stress, signal transduction, transporter, transcription factor, nucleotide metabolism, RNA processing, and protein metabolism (Fig. 6). Primary DEGs belonged to five functional groups: carbohydrate metabolism, signal transduction, nucleotide metabolism, response to stress and transporter, suggesting that the occurrence of high Pn in rice might be closely related to these functional and regulatory pathways. Furthermore, four genes associated with photosynthesis were differentially expressed between Zhefu802 and Chl-8, implying that in addition to genes associated with photosynthesis, many genes or multiple metabolic pathways may play significant roles in high photosynthetic efficiency in rice.

Analysis of DEGs involved in the regulation of photosynthesis

Physio-biochemical analysis of leaves indicated that multiple metabolic pathways regulated differences in photosynthesis between Zhefu802 and Chl-8. So transcriptome analysis focused on DEGs involved in the regulation of photosynthesis. Of particular interest were several key DEGs that are known to be involved with photosynthesis, controlling synthesis and disintegration of ATP, antioxidant properties, nitrate transportation and photorespiration. As shown in Fig. 7, expression of two DEGs encoding ubiquinone and plastocyanin respectively, directly participated in transport

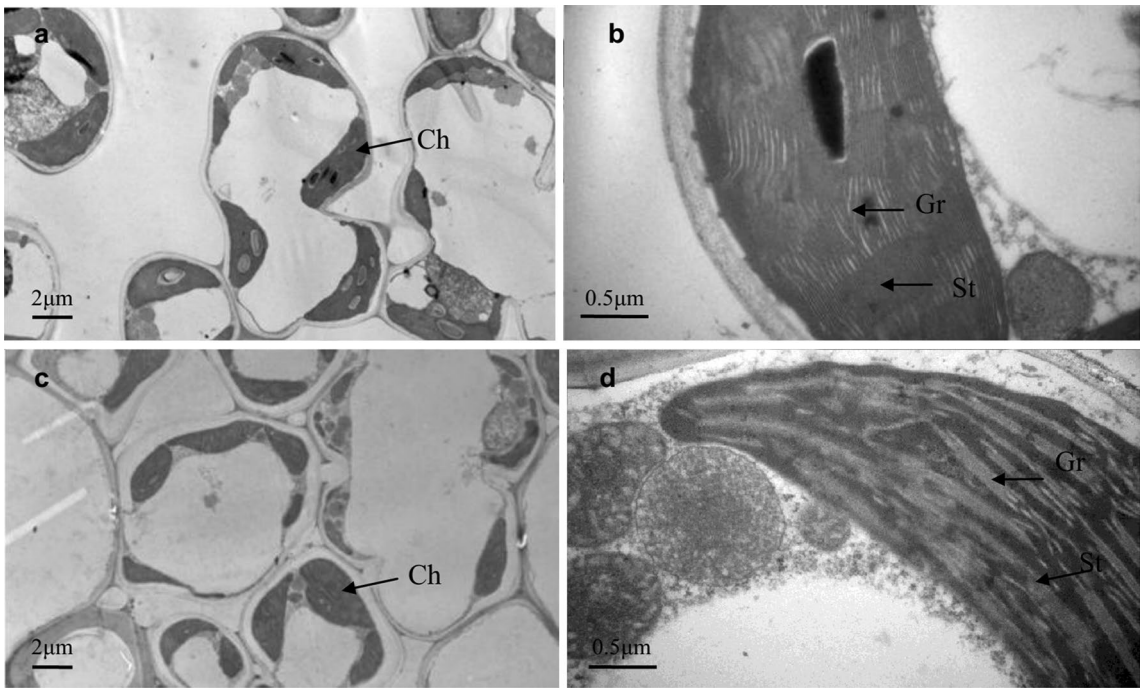

Fig. 3 Comparison of subcellular structures in the youngest fully expanded leaves of Zhefu802 and Chl-8. **a**, **b** Subcellular structures of leaf and cross-section of chloroplast in Zhefu802. **c**, **d** Subcellular structures of leaf and cross-section of chloroplast in Chl-8. *Gr* granal thylakoid, *St* stromal thylakoid

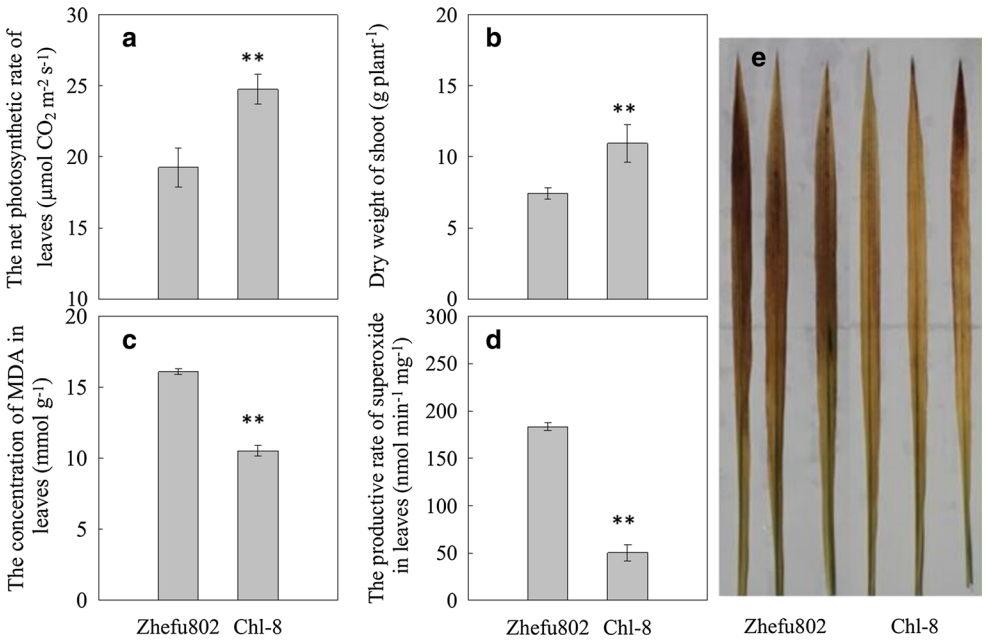

Fig. 4 Photosynthesis, dry matter accumulation and oxidative concentration of Zhefu802 and Chl-8. **a** Net photosynthetic rate of two varieties. **b** Dry matter accumulation of two varieties. **c** Malondialdehyde (MDA) concentration in leaves of two varieties. **d** Productive rate of superoxide in leaves of two varieties. **e** H_2O_2 concentration in leaves of two varieties, H_2O_2 was visualized as a reddish-brown coloration. Vertical bars denote standard deviations ($n = 6$). The significance of differences compared with Zhefu802 is indicated with two asterisks (LSD, $P < 0.01$)

electrons to photosystem I, and were significantly up-regulated, while *Ohp* encoding one-helix protein, light stress-responsive protein, was more highly expressed in Chl-8 compared with Zhefu802. Expression of a DEG encoding ATPase that catalyzes the hydrolysis of ATP was up-regulated, whereas expression of another DEG encoding apyrase, which catalyzes the hydrolysis of phosphoanhydride bonds of nucleoside tri- and di-phosphates into monophosphates, was down-regulated in Chl-8. The expression of a DEG encoding the pyrophosphate-energized proton pump was down-regulated in Chl-8. The expression levels of two DEGs of thiolation protein were enhanced, and expression

Table 2 Chlorophyll fluorescence analysis in leaves of Zhefu802 and Chl-8

Material	F_v/F_m	ΦPS II	1-qP	NPQ
Zhefu802	0.75b	0.37b	0.49a	0.23b
Chl-8	0.80a	0.45a	0.39b	0.61a

Different lower-case letters indicate statistically significant differences ($P < 0.05$) between Zhefu802 and Chl-8

Table 3 Assessment of data from transcriptome sequencing on an Illumina High-Seq 2500 platform

Samples	Read number	Base number	GC content (%)	% ≥ *Q*30
Zhefu802-1	26,528,266	6,681,256,954	55.37	87.37
Zhefu802-2	24,503,439	6,170,411,945	55.40	87.31
Zhefu802-3	24,813,452	6,250,417,521	54.32	87.61
Chl-8-1	23,801,718	5,995,805,975	55.09	87.23
Chl-8-2	25,968,383	6,540,622,834	55.43	86.65
Chl-8-3	25,968,383	6,318,191,172	55.39	87.30

Table 4 Statistics of the sequences mapped to the complete set of CDS from Rice_9311 (http://rice.genomics.org.cn/rice2/link/download.jsp)

Samples	Total reads	Mapped reads	Mapped ratio (%)
Zhefu802-1	53,056,532	45,005,435	84.83
Zhefu802-2	49,006,878	41,348,272	84.37
Zhefu802-3	49,626,904	42,452,812	85.54
Chl-8-1	47,603,436	40,723,773	85.55
Chl-8-2	51,936,766	43,927,791	84.58
Chl-8-3	50,169,192	42,530,348	84.77

Table 5 Distribution of single nucleotide polymorphism (SNP) along the chromosomes

	SNP number	Chromosome length (bp)	Abundance (1/10 kb)
Chromosome01	10,509	46,148,067	2.28
Chromosome02	7032	36,461,309	1.93
Chromosome03	7772	39,893,827	1.95
Chromosome04	5580	36,479,295	1.53
Chromosome05	4101	30,648,699	1.34
Chromosome06	4524	31,571,114	1.43
Chromosome07	4157	28,264,064	1.47
Chromosome08	4302	31,235,534	1.38
Chromosome09	2609	22,417,016	1.16
Chromosome10	4308	24,583,340	1.75
Chromosome11	3590	30,129,896	1.19
Chromosome12	3889	26,138,844	1.49

of *AMR1* (ascorbic acid mannose pathway regulator 1) was significantly down-regulated in Chl-8. *AMR1* transcripts accumulated with a concomitant decrease in AsA and decreased with increased light intensity. The expression of two *GST* (Glutathione transferase) genes decreased while the expression of another *GST* gene significantly increased. These differences in antioxidant gene expression might contribute to the greater ability of Chl-8 to scavenge reactive oxygen species compared with Zhefu802. Three DEGs were found in the nitrate transport pathway, indicating the variance of nitrogen metabolism between Zhefu802 and Chl-8. One DEG was detected in the photorespiration pathway. Ten key DEGs involved in photosynthesis-related processes were selected for qRT-PCR analysis. In general, the qRT-PCR data were consistent with the Illumina sequencing results, suggesting that the RNA-Seq data are reliable (Fig. 8).

Discussion

By 2015, more than 182 leaf color genes had been identified, and about 30 genes of these genes were derived from rice (Liu et al. 2015). It was demonstrated that these genes were involved in the chlorophyll metabolism and chloroplast development (Kong et al. 2016). The chlorophyll metabolic pathway and mechanisms of chloroplast development were studied systematically by both biochemical and genetic approaches. However, the effect of pigment metabolism and leaf structure on photosynthesis is still vague. In our experiment, the Pn of Chl-8 was significantly higher than that of Zhefu802, although chlorophyll content was significantly higher in Zhefu802 (Fig. 2). However, in paddy field, the yield of Zhefu802 is higher than that of Chl-8 (data not show). Complex factors impact consistency between photosynthesis and yield, such as growth duration, carbohydrate transportation, respiration-based consumption and leaf area. The significance of studying high photosynthetic efficiency in Chl-8 is not weakened by this phenomenon. Previous study shown leaf of Chl-8 was more tolerant to high light than Zhefu802 (Zhao et al. 2016). But so far, the high photosynthesis mechanisms of deficient chlorophyll leaf have not been characterized at the genetic level. We compared the biochemical characteristics and gene expression profiles of two rice genotypes to reveal the underlying molecular mechanism related to high photosynthetic efficiency.

Leaf color and high photosynthetic efficiency

The antenna is composed of specialized membrane-bound light harvesting pigment–protein complexes, in which chlorophylls and carotenoids are organized in a very ordered manner at significant densities (Pascal et al. 2005). In contrast to chlorophyll's essential energy-harvesting role,

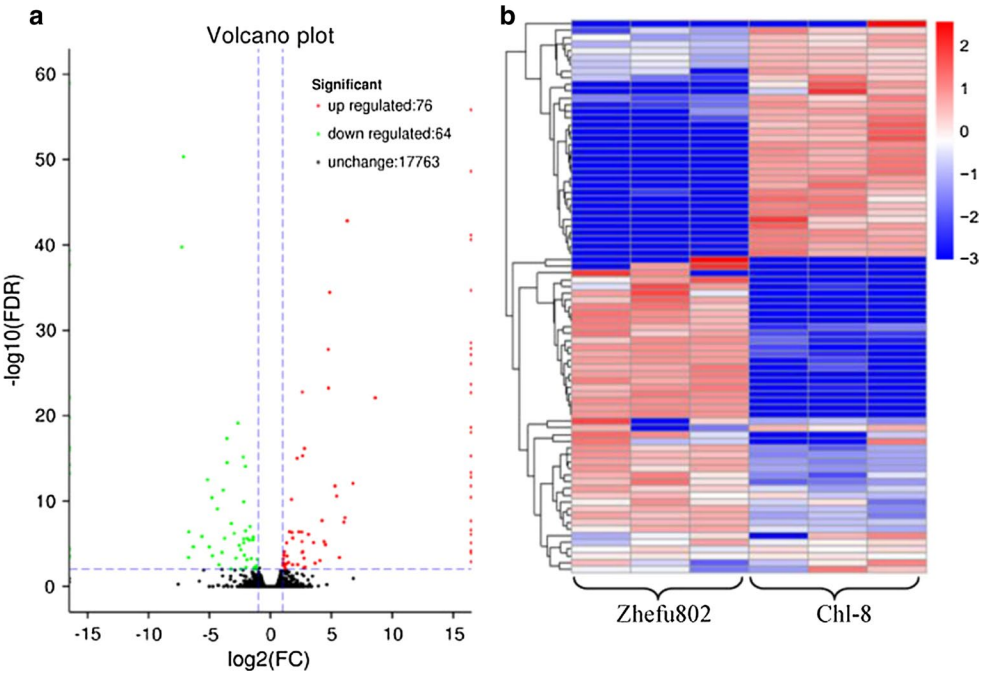

Fig. 5 Volcano plot and hierarchical clustering of differentially expressed genes between Zhefu802 and Chl-8. **a** Volcano plot illustrating the differentially expressed probes in Zhefu802 versus Chl-8. The *X*-axis represents the fold change in Chl-8 compared to Zhefu802 (on a $\log_2$ scale), and the *Y*-axis represents the negative log10-transformed *P* values ($P \leq 0.01$) of the *t* test for finding differences between the samples. **b** Hierarchical clustering of differentially expressed genes, fragments per kilobase of transcript per million fragments mapped (FPKM), $\log_2$ FPKM of differentially expressed genes were calculated, and the data were clustered. A scale indicating the color assigned to $\log_2$ FPKM is shown to the right of the cluster

Table 6 Functional classification of differentially expressed genes associated with enriched GO terms

GO.ID	Term	Gene number	KS
A. Biological process			
GO:0055114	Oxidation–reduction process	10	1.30E−06
GO:0006629	Lipid metabolic process	6	2.10E−05
GO:0006355	Regulation of transcription, DNA-dependent	10	3.90E−05
GO:0009651	Response to salt stress	7	0.00087
GO:0006468	Protein phosphorylation	6	0.00102
GO:0006810	Transport	16	0.01134
GO:0005975	Carbohydrate metabolic process	5	0.0224
GO:0055085	Transmembrane transport	8	0.03409
GO:0009416	Response to light stimulus	7	0.03909
B. Cellular component			
GO:0005886	Plasma membrane	6	1.50E−11
GO:0005634	Nucleus	15	6.90E−11
GO:0016021	Integral to membrane	11	2.70E−05
GO:0016023	Cytoplasmic membrane-bounded vesicle	27	0.00264
GO:0009507	Chloroplast	5	0.01258
C. Molecular function			
GO:0005524	ATP binding	11	5.70E−06
GO:0009055	Electron carrier activity	5	0.00045
GO:0004674	Protein serine/threonine kinase activity	6	0.00085
GO:0005515	Protein binding	11	0.00233
GO:0016757	Transferase activity	5	0.01162
GO:0016705	Oxidoreductase activity	6	0.01789

Differentially expressed genes with fold change ≥ 2 and FDR (false discovery rate) ≤ 0.01 are classified here. Only terms with more than five genes/transcripts were listed here

KS Kolmogorov–Smirnov test

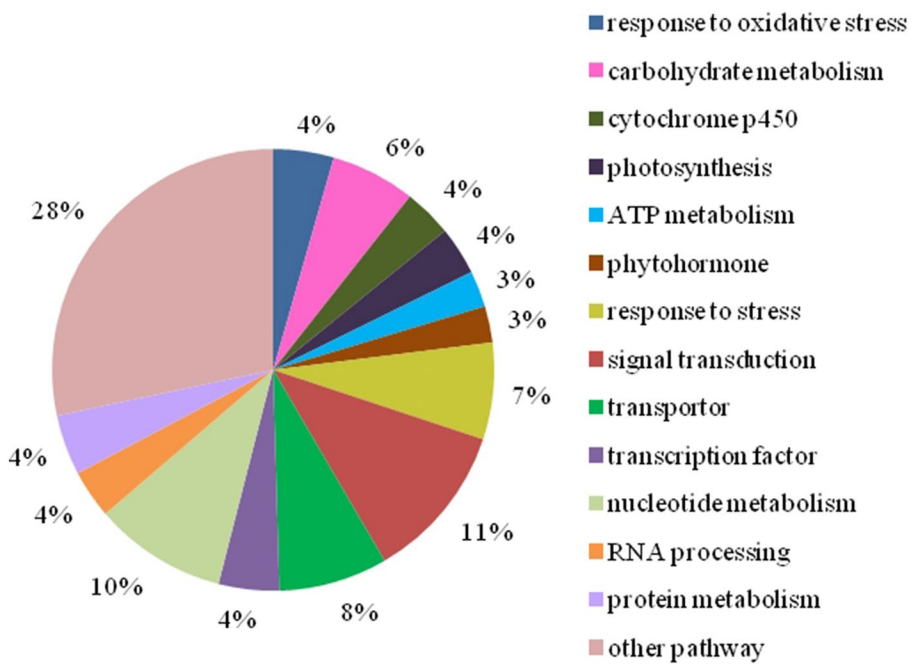

Fig. 6 Functional classification and distribution of 140 differentially expressed genes. The data in the figure represent the percentage of each category

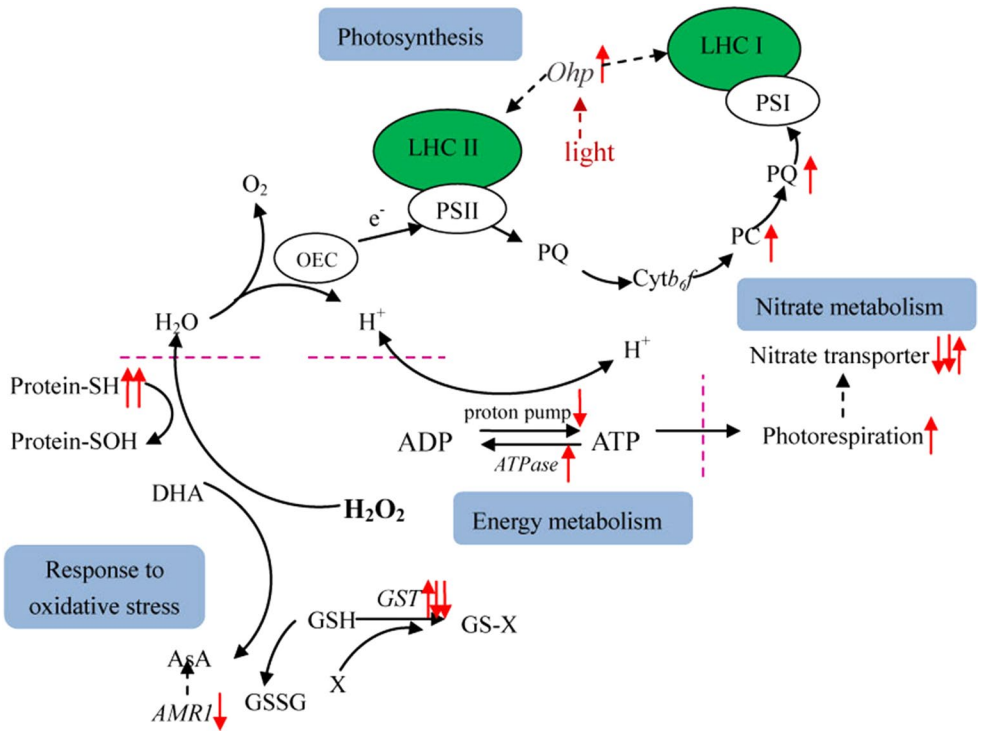

Fig. 7 Key differentially expressed genes in biological process between Zhefu802 and Chl-8. Up arrows designate up-regulation of the genes and down arrows indicate down-regulated genes. The number of arrows specifies the number of genes. *PSI(II)* photosynthetic system I(II), *LHCI(II)* light harvest complex of PSI(II), *OEC* oxygen evolution complex, *PQ* ubiquinone, *PC* plastocyanin, *AsA* ascorbic acid, *DHA* dehydroascorbic acid, *AMR1* ascorbic acid mannose pathway regulator 1, *GSH* glutathione, *GSSG* oxidized glutathione, *GST* glutathione s-transferase, *X* toxic oxide

chlorophyll and its intermediate derivatives can also interact with oxygen molecules, giving rise to toxic singlet oxygen radicals (Sakuraba et al. 2013). Carotenoids collect light energy to drive photosynthetic processes and their role in protecting the photosynthetic apparatus against destructive effects of excessive light and toxic oxides are well established (Siefermann-Harms 1987). Total chlorophyll, chlorophyll *a*:*b* and chlorophylls:carotenoids all correlated significantly with saturated light intensity (Marschall and Proctor 2004). In this study, the Chlorophyll *a*, Chlorophyll *b*, and carotenoid contents of Chl-8 were significantly lower than those of Zhefu802; however, chlorophyll *a*:*b* and ratio of carotenoid to chlorophyll in Chl-8 were higher than those in Zhefu802. These results were correlated with

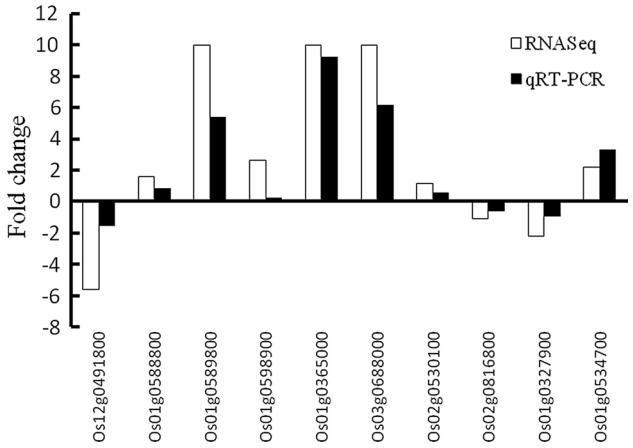

Fig. 8 qRT-PCR results confirmed differentially expressed transcripts identified by RNA-Seq. Ten key genes were selected for qRT-PCR analysis for validation. These genes were selected on the basis of their role in photosynthesis-related processes

higher expression levels of corresponding genes detected in our transcriptome data. The expression of *Ohp*, encoding one-helix proteins which locates light harvest system and belongs to the chlorophyll *a*/*b*-binding family and that play roles in photoprotection and pigment metabolism, was up-regulated in Chl-8 compared with Zhefu802. (Andersson et al. 2003; Umate 2010). Three DEGs were found in the nitrate transport pathway, indicating a difference in nitrogen metabolism between Zhefu802 and Chl-8. Fan et al. (2016) reported that overexpression of a pH-sensitive nitrate transporter (OsNRT2.3b) in rice increases nitrogen use efficiency. Four cytochrome P450 genes were differentially expressed between Zhefu802 and Chl-8. Cytochromes P450 are hemoproteins encoded by a superfamily of genes, which almost ubiquitously existed in a wide range of species. Cytochromes P450 is a kind of external monooxygenase and thus receives the necessary electrons for oxygen cleavage and substrate hydroxylation from different redox partners (Morant et al. 2003; Hannemann et al. 2007). Many enzymes involved in chlorophyll and carotenoid biosynthesis belong to the cytochrome P450 group (Lange and Ghassemian 2003; Quinlan et al. 2007; Christ et al. 2013).

The leaf color formation is not only greatly affected by pigment metabolism but also affected by the activity of chloroplast development (Yang et al. 2015). To characterize the structural basis of the leaf color phenotype, cross-sections of rice leaf and ultrastructures of chloroplast were compared (Figs. 2, 3). There was a lower leaf thickness of Chl-8 compared to Zhefu802. No significant differences in mesophyll tissue thickness and the size of mesophyll cells between the two cultivars were observed (Fig. 2). Chloroplasts in Zhefu802 developed an abundant membrane system (Fig. 3b). However, the appressed and non-appressed thylakoid membrane was less in Chl-8 (Fig. 3d). Thylakoid with greater membrane stacking have higher D1 protein degradation and are more susceptible to photoinhibition (Anderson and Aro 1994; Anderson et al. 2012; Jiang et al. 2011). The ultrastructure of chloroplast suggests that Zhefu802 may be more susceptible to photoinhibition. The results derived from RNA-Seq analysis were in line with the significant difference of leaf structure and chloroplast ultrastructures between Zhefu802 and Chl-8. Five DEGs were classified into a functional group named chloroplast (GO:0009507). These results suggested that pigment metabolism and leaf and chloroplast development affected leaf color formation along with regulation of photosynthetic efficiency.

DEGs involved in high photosynthetic efficiency

There were significantly higher levels of F_v/F_m, Φ_{PSII} and NPQ, and a clear lower level of 1-qP in the leaves of Chl-8 compared with Zhefu802, which indicates that Chl-8 exhibits more robust capacity for electron transport and dissipated excessive excited energy via heat. Expression of two DEGs encoding ubiquinone and a plastocyanin protein, respectively, directly transport electrons to Photosystem I, were up-regulated in Chl-8 compared with Zhefu802. The DEGs encoding ubiquinone and a plastocyanin protein locate chromosome 1 and 2, respectively. *Ohp* encoding one-helix protein, a light stress-responsive protein, was more highly expressed in Chl-8. *Ohp* locates chromosome 1 and its translation is induced by high light intensity. In this study, seven DEGs classified into a functional group named response to light stimulus (GO:0009416), suggesting light conditions might affect the differential expression patterns. To counter photodamage, plants have developed multiple photoprotective mechanisms, including photorespiration and NPQ (Kasajima et al. 2011). The expression of one DEG involved in photorespiration was up-regulated in Chl-8. Nitrate assimilation in both dicotyledonous and monocotyledonous species depends on photorespiration (Rachmilevitch et al. 2004; Bloom 2015). The difference in nitrate assimilation was observed in RNA-Seq analysis. 6% DEGs were classed into the carbohydrate metabolism category (Fig. 6). It is possible that CO_2 assimilation and carbohydrate metabolism are affected by energy metabolism. In the aspect of energy metabolism, ATPase catalyzes the hydrolysis of ATP and was up-regulated, whereas apyrase catalyzes the hydrolysis of phosphoanhydride bonds of nucleoside tri- and di-phosphates into monophosphates and was down-regulated. The expression of a gene encoding the pyrophosphate-energized proton pump was down-regulated. These DEGs involved with electron transport, photorespiration and energy metabolism process might contribute to high photosynthetic efficiency in Chl-8.

Generation of toxic oxides linked with photosynthetic efficiency

Photosynthesis may not always be greater in plants with high light harvesting capacity, given that excess light can subject plants to oxidative stress when their ability to dissipate heat is insufficient (Ware et al. 2015). High levels of NPQ and low chlorophyll content were favorable in reducing the accumulation of toxic oxides in Chl-8. The generation of high levels of toxic oxides was a contributing factor in the damaging of the photosynthetic apparatus and photoinhibition (Suzuki et al. 2012; Roach et al. 2015). The significant decreases in toxic oxides, including MDA, O_2^- and H_2O_2, in Chl-8 were measured, which might be associated with differences in the expression of antioxidant genes. 4% DEGs were assigned to the response to oxidative stress category. The expression level of two genes of the thiolation protein was enhanced and the expression level of *AMR1* (ascorbic acid mannose pathway regulator 1) was down-regulated. *AMR1* transcripts accumulated with a concomitant decrease in ascorbic acid (Zhang et al. 2009). Two *GST* (Glutathione transferase) genes had decreased expression and another *GST* gene had an increase in expression. Glutathione transferase and ascorbic acid are primary antioxidants in leaves (Frova 2003; Moons 2003; Guo et al. 2005; Gallie 2013). These DEGs might contribute to an increased ability to scavenge reactive oxygen species in Chl-8 compared to Zhefu802. The importance of the antioxidant network in maintaining high rates of photosynthesis has been demonstrated in many studies (Asada 2006; Bonnecarrère et al. 2011; Foyer and Shigeoka 2011). Toxic oxides are signal molecules that play vital roles in the response to biotic and abiotic stress in plants (Apel and Hirt 2004; Foyer and Shigeoka 2011). 7% DEGs were assigned to response to stress, and 11% DEGs were assigned to signal transduction (Fig. 6). This indicated that there was a significant difference in stress resistance between Chl-8 and Zhefu802, which may be associated with high photosynthetic efficiency.

High photosynthetic efficiency involves coordinated regulation of multiple pathways

Physiological and transcriptome analysis of a near-isogenic line, Chl-8 (with pale-green leaf and high photosynthesis), and its parental line, Zhefu802 (with dark-green leaf and low photosynthesis), support the notion that photosynthesis is controlled by delicate but complex genetic networks. Notably, in addition to DEGs directly involved in photosynthesis, other DEGs implicated in the response to oxidative stress, energy metabolism and nitrate metabolism co-regulated photosynthetic efficiency in rice (Fig. 7). DEGs categorized to signal transduction supported the regulation. Suitable chlorophyll content, ratio of chlorophyll to carotenoid, and thylakoid membrane system also promoted high photosynthetic efficiency. Further refinement of Chl-8 genetic information may eventually help with cloning and engineering the major genes underlying the mechanism in high photosynthetic efficiency.

Author contribution statement GF and XZ conceived, designed research and wrote the manuscript; XZ, TC, CZ and BF accomplished all experiments involved in this paper. LT offered key idea and scientific guidance for this research. LT revised the manuscript critically for important intellectual content. BF and XZ sorted out and analyzed all materials in this research. All authors listed in here contributed and approved the manuscript.

Acknowledgements We thank Chen Zheng and Wang Yi for valuable advice on RNA-Seq analysis and quantitative RT-PCR. We thanks for assistance from Meiqin Shao, Xueqin Yang and Yongjie Yang from China National Rice Research Institution during research process.

Compliance with ethical standards

Funding This work was funded by the National Natural Science Foundation of China (Grant nos. 31501264, 31561143003 and 31671619), National Food Science and Technology Project (2016YFD0300208), Zhejiang Provincial Natural Science Foundation, China (LQ15C130003), the China National Rice Research Institute (Grant no. 2014RG004-4), and the MOA Special Fund for Agro-scientific Research in the Public Interest of China (Grant no. 201203029).

Conflict of interest All authors of this paper declare that the research was not involved with any commercial or financial relationships that could form a potential conflict of interest.

References

Anders S, Huber W (2010) Differential expression analysis for sequence count data. Genome Biol 11:106

Anderson JM, Aro EM (1994) Grana stacking and protection of photosystem II in thylakoid membranes of higher plant leaves under sustained high irradiance: an hypothesis. Photosynth Res 41:315–326

Anderson JM, Horton P, Kim EH, Chow WS (2012) Towards elucidation of dynamic structural changes of plant thylakoid architecture. Philos Trans R Soc B 367:3515–3524

Andersson U, Heddad M, Adamska I (2003) Light stress-induced one-helix protein of the chlorophyll *a*/*b*-binding family associated with photosystem I. Plant Physiol 132:811–820

Apel K, Hirt H (2004) Reactive oxygen species: metabolism, oxidative stress, and signal transduction. Annu Rev Plant Biol 55:373–399

Asada K (2006) Production and scavenging of reactive oxygen species in chloroplasts and their functions. Plant Physiol 141:391–396

Benjamini Y, Hochberg Y (1995) Controlling the false discovery rate: a practical and powerful approach to multiple testing. J R Stat Soc Ser B (Methodological) 57:289–300

Bloom AJ (2015) Photorespiration and nitrate assimilation: a major intersection between plant carbon and nitrogen. Photosynth Res 123:117–128

Bonnecarrère V, Borsani O, Díaz P, Capdevielle F, Blanco P, Monza J (2011) Response to photoxidative stress induced by cold in japonica rice is genotype dependent. Plant Sci 180:726–732

Boveris A (1984) Determination of the production of superoxide radicals and hydrogen peroxide in mitochondria. Methods Enzymol 105:429–435

Bozzola JJ, Russell LD (1999) Electron microscopy: principles and techniques for biologists. Jones and Bartlett Publisher, Burlington, Massachusetts

Cao XN, Ma F, Xu TT, Wang JJ, Liu SC, Li GH, Su QQ, Zhi J, Na XF (2016) Transcriptomic analysis reveals key early events of narciclasine signaling in Arabidopsis root apex. Plant Cell Rep 35:2381–2401

Chaitanya KK, Naithani SC (1994) Role of superoxide, lipid peroxidation and superoxide dismutase in membrane perturbation during loss of viability in seeds of *Shorea robusta* Gaertn. f. New Phytol 126:623–627

Christ B, Süssenbacher I, Moser S, Bichsel N, Egert A, Müller T, Kräutler B, Hörtensteiner S (2013) Cytochrome P450 CYP89A9 is involved in the formation of major chlorophyll catabolites during leaf senescence in Arabidopsis. Plant Cell 25(5):1868–1880

Dionisio-Sese ML, Tobita S (1998) Antioxidant responses of rice seedlings to salinity stress. Plant Sci 135:1–9

Fan XR, Tang Z, Tan YW, Zhang Y, Luo BB, Yang M, Lian XM, Shen QR, Miller AJ, Xu GH (2016) Overexpression of a pH-sensitive nitrate transporter in rice increases crop yields. Proc Natl Acad Sci USA 113:7118–7123

Feng BH, Yang Y, Shi YF, Shen HC, Wang HM, Huang QN, Xu X, Lu XG, Wu JL (2013) Characterization and genetic analysis of a novel rice spotted-leaf mutant HM47 with broad-spectrum resistance to xanthomonas oryzae pv. oryzae. J Integr Plant Biol 55:473–483

Foyer CH, Shigeoka S (2011) Understanding oxidative stress and antioxidant functions to enhance photosynthesis. Plant Physiol 155:93–100

Frova C (2003) The plant glutathione transferase gene family: genomic structure, functions, expression and evolution. Physiol Plant 119:469–479

Gallie DR (2013) The role of L-ascorbic acid recycling in responding to environmental stress and in promoting plant growth. J Exp Bot 64:433–443

Gu J, Yin X, Stomph TJ, Struik PC (2014) Can exploiting natural genetic variation in leaf photosynthesis contribute to increasing rice productivity? A simulation analysis. Plant Cell Environ 37:22–34

Guo Z, Tan H, Zhu Z, Lu S, Zhou B (2005) Effect of intermediates on ascorbic acid and oxalate biosynthesis of rice and in relation to its stress resistance. Plant Physiol Biochem 43:955–962

Hannemann F, Bichet A, Ewen KM, Bernhardt R (2007) Cytochrome P450 systems—biological variations of electron transport chains. BBA Gen Subj 1770:330–344

Jiang CD, Wang X, Gao HY, Shi L, Chow WS (2011) Systemic regulation of leaf anatomical structure, photosynthetic performance, and high-light tolerance in sorghum. Plant Physiol 155:1416–1424

Kasajima I, Ebana K, Yamamoto T, Takahara K, Yano M, Kawai-Yamada M (2011) Molecular distinction in genetic regulation of nonphotochemical quenching in rice. Proc Natl Acad Sci USA 108:13835–13840

Kim D, Pertea G, Trapnell C, Pimentel H, Kelley R, Salzberg SL (2013) TopHat2: accurate alignment of transcriptomes in the presence of insertions, deletions and gene fusions. Genome Biol 14:R36

Kong WY, Yu XW, Chen HY, Liu LL, Xiao YJ, Wang YL, Wang CL, Lin Y, Yu Y, Wang CM, Jiang L, Zhai HQ, Zhao ZG, Wan JM (2016) The catalytic subunit of magnesium-protoporphyrin IX monomethyl ester cyclase forms a chloroplast complex to regulate chlorophyll biosynthesis in rice. Plant Mol Biol 92:177–191

Lange BM, Ghassemian M (2003) Genome organization in *Arabidopsis thaliana*: a survey for genes involved in isoprenoid and chlorophyll metabolism. Plant Mol Biol 51:925–948

Li H, Handsaker B, Wysoker A (2009) The sequence alignment/map format and SAMtools. Bioinformatics 25:2078–2079

Liu J, Wang J, Yao X, Dong X, Chen W (2015) Fine mapping and photosynthetic characteristics of the lower chlorophyll *b* 1 mutant in rice (*Oryza sativa* L.). Plant Breed 134:661–667

Long SP, Marshall-Colon A, Zhu XG (2015) Meeting the global food demand of the future by engineering crop photosynthesis and yield potential. Cell 161:56–66

Marschall M, Proctor MCF (2004) Are bryophytes shade plants? Photosynthetic light responses and proportions of chlorophyll *a*, chlorophyll *b* and total carotenoids. Ann Bot Lond 94:593–603

Maxwell K, Johnson GN (2000) Chlorophyll fluorescence—a practical guide. J Exp Bot 51:659–668

Moons A (2003) Osgstu3 and osgtu4, encoding tau class glutathione S-transferases, are heavy metal- and hypoxic stress-induced and differentially salt stress-responsive in rice roots 1. FEBS Lett 553:427–432

Morant M, Bak S, Møller BL, Werck-Reichhart D (2003) Plant cytochromes P450: tools for pharmacology, plant protection and phytoremediation. Curr Opin Biotechnol 14:151–162

Pascal AA, Liu ZF, Broess K, Van OB, Van AH, Wang C, Horton P, Robert B, Chang WR, Ruban A (2005) Molecular basis of photoprotection and control of photosynthetic light-harvesting. Nature 436:134–137

Quinlan RF, Jaradat TT, Wurtzel ET (2007) Escherichia coli as a platform for functional expression of plant P450 carotene hydroxylases. Arch Biochem Biophys 458:146–157

Rachmilevitch S, Cousins AB, Bloom AJ (2004) Nitrate assimilation in plant shoots depends on photorespiration. Proc Natl Acad Sci USA 101(31):11506–11510

Roach T, Na CS, Krieger-Liszkay A (2015) High light-induced hydrogen peroxide production in *Chlamydomonas reinhardtii* is increased by high CO_2 availability. Plant J 81:759–766

Ruzin SE (1999) Plant microtechnique and microscopy, vol 198. Oxford University Press, New York

Sage TL, Sage RF (2009) The functional anatomy of rice leaves: implications for refixation of photorespiratory CO_2 and efforts to engineer C_4 photosynthesis into rice. Plant Cell Physiol 50:756–772

Sakuraba Y, Rahman ML, Cho SH, Kim YS, Koh HJ, Yoo SC, Paek NC (2013) The rice faded green leaf locus encodes protochlorophyllide oxidoreductase B and is essential for chlorophyll synthesis under high light conditions. Plant J 74:122–133

Sartory DP, Grobbelaar JU (1984) Extraction of chlorophyll *a* from freshwater phytoplankton for spectrophotometric analysis. Hydrobiologia 114:177–187

Siefermann-Harms D (1987) The light-harvesting and protective functions of carotenoids in photosynthetic membranes. Physiol Plant 69:561–568

Suzuki N, Koussevitzky S, Mittler R, Miller G (2012) ROS and redox signalling in the response of plants to abiotic stress. Plant Cell Environ 35:259–270

Thordal-Christensen H, Zhang Z, Wei Y, Collinge DB (1997) Subcellular localization of H_2O_2 in plants. H_2O_2 accumulation in papillae and hypersensitive response during the barley—powdery mildew interaction. Plant J 11:1187–1194

Umate P (2010) Genome-wide analysis of the family of light-harvesting chlorophyll *a*/*b*-binding proteins in arabidopsis and rice. Plant Signal Behav 5:1537–1542

Wakasa Y, Oono Y, Yazawa T, Hayashi S, Ozawa K, Handa H, Matsumoto T, Takaiwa F (2014) RNA sequencing-mediated

transcriptome analysis of rice plants in endoplasmic reticulum stress conditions. BMC Plant Biol 14:101

Wang DY, Xu CM, Chen S, Tiao LX, Zhang XF (2012) Photosynthesis and dry matter accumulation in different chlorophyll-deficient rice lines. J Integr Agric 11:397–404

Wang JL, Lei CL, Wu FQ, Lin QB, Liu YQ, Liu LL, Jiang L (2013) A knockdown mutation of yellow-green leaf 2 blocks chlorophyll biosynthesis in rice. Plant Cell Rep 32:1855–1867

Ware MA, Belgio E, Ruban AV (2015) Photoprotective capacity of non-photochemical quenching in plants acclimated to different light intensities. Photosynth Res 126:261–274

Wu ZM, Zhang X, He B, Diao LP, Sheng SL, Wang JL, Guo XP, Su N, Wang LF, Jiang L (2007) A chlorophyll-deficient rice mutant with impaired chlorophyllide esterification in chlorophyll biosynthesis. Plant Physiol 145:29–40

Wu Q, Chen Z, Sun W, Deng T, Chen M (2016) De novo sequencing of the leaf transcriptome reveals complex light-responsive regulatory networks in *Camellia sinensis* cv. *Baijiguan*. Front Plant Sci 7:332

Yang W, Yoon J, Choi H, Fan Y, Chen R, An G (2015) Transcriptome analysis of nitrogen-starvation-responsive genes in rice. BMC Plant Biol 15:1–12

Zhang W, Lorence A, Gruszewski HA, Chevone BI, Nessler CL (2009) AMR1, an arabidopsis gene that coordinately and negatively regulates the mannose/L-galactose ascorbic acid biosynthetic pathway. Plant Physiol 150:942–950

Zhao X, Chen T, Feng B, Zhang C, Peng S, Zhang X, Fu G, Tao L (2016) Non-photochemical quenching plays a key role in light acclimation of rice plants differing in leaf color. Front Plant Sci 7:1968